

# TEMPERATURE CHARACTERISTICS OF A THIN AND COMPACT LINEAR SWITCHED RELUCTANCE MOTOR

M.N. Maslan<sup>1</sup> and K. Sato<sup>2</sup>

<sup>1</sup>Faculty of Manufacturing Engineering,  
Universiti Teknikal Malaysia Melaka, Hang Tuah Jaya, 76100 Durian  
Tunggal, Melaka, Malaysia.

<sup>2</sup>Department of Mechanical Engineering,  
Toyohashi University of Technology, 1-1 Hibarigaoka,  
Tempaku-cho, Toyohashi, 441-8580 Aichi, Japan.

Corresponding Author's Email: [nazmin@utem.edu.my](mailto:nazmin@utem.edu.my)

**Article History:** Received 5 September 2019; Revised 23 December 2019;  
Accepted 9 April 2020

**ABSTRACT:** The human body shows a non-linear and dynamic behavior under different vibration conditions that occur while travelling, walking and performing other activities. Thus, it becomes necessary to study effects on the human body that lead to different types of body pain and discomfort. In this study, an attempt has been made to find out natural frequencies and mode shapes of an Indian male subject in sitting posture without backrest using FEM approach. The results will be helpful in the designing of products for human use like automobile seats and machine parts to minimize the effect of vibrations on human body. A 3-D CAD model of human subject was generated using physical dimensions and anthropometric data available in the existing literature. A CAD model of the human body was segmented into a simple model using segments of ellipsoidal shape. As observed from this study, at 2.8 Hz maximum deformation of 56 mm occurred at head segment and with the increase in natural frequency it started diverting to lower arms. At 18.7 Hz, maximum deformation (124 mm) occurred at lower arms of human subject. Also, no deformation occurred at lower body segments below hip joint. The results obtained are in validation with the existing literature.

**KEYWORDS:** *Modal Analysis; Human Body; Natural Frequency; FEM; Sitting Posture*

## 1.0 INTRODUCTION

Electromagnetic linear motors are examples of linear drive mechanisms that have the capability to achieve high thrust performance suitable for high-speed and high-precision system [1]. However, linear motors depend on permanent magnets (PMs), which

have powerful attractive forces, thereby making assembly and disassembly difficult. A linear switched reluctance motor (LSRM) is free from the attractive force of the magnets and therefore, able to realize a thin and compact structure. Various configurations of LSRMs have been developed over the past few decades [2–6]. Although LSRMs have been studied for many applications such as elevators [7–10], railways [11–12], generator [13], automatic door [14–15], biomedical [16] and vehicle active suspension system [17], they are more suitable for compact direct drive mechanisms. Apart from the study on high-precision performance [18–19], it is utmost important to examine the temperature characteristics of the LSRM [1]. This is because temperature changes are considered undesirable in high-precision systems.

This paper describes the temperature characteristics of the developed LSRM using thermography. Although various precision tracking experiments were carried out previously [20], the temperature rise at the time of driving remains unclear. Therefore, the temperature rise during motion are examined experimentally. The remainder of this paper is organized as follows. In Section 2, the experimental setup and conditions are explained. Section 3 describes the temperature characteristic of the LSRM and its discussion. Finally, Section 4 presents the conclusions of this study.

## **2.0 METHODOLOGY**

### **2.1 Experimental Setup**

In order to know the extent of the temperature rise at the time of driving, the temperature of the stator coils by the motion control system in [20] was measured using thermography. Figure 1 shows the schematic diagram of the experimental setup. A digital signal processing (DSP) system provided the driving signals to be applied to the commercial current amplifiers. These amplifiers are used to drive each phase of the coil. Simultaneously, the DSP system obtains the displacement of the mover from the linear encoder. In addition, an infrared camera is used to measure the temperature of stator coils. It is connected to a controller that stores the data and receives input from the console. Thermal images can also be viewed through the monitor in real-time.

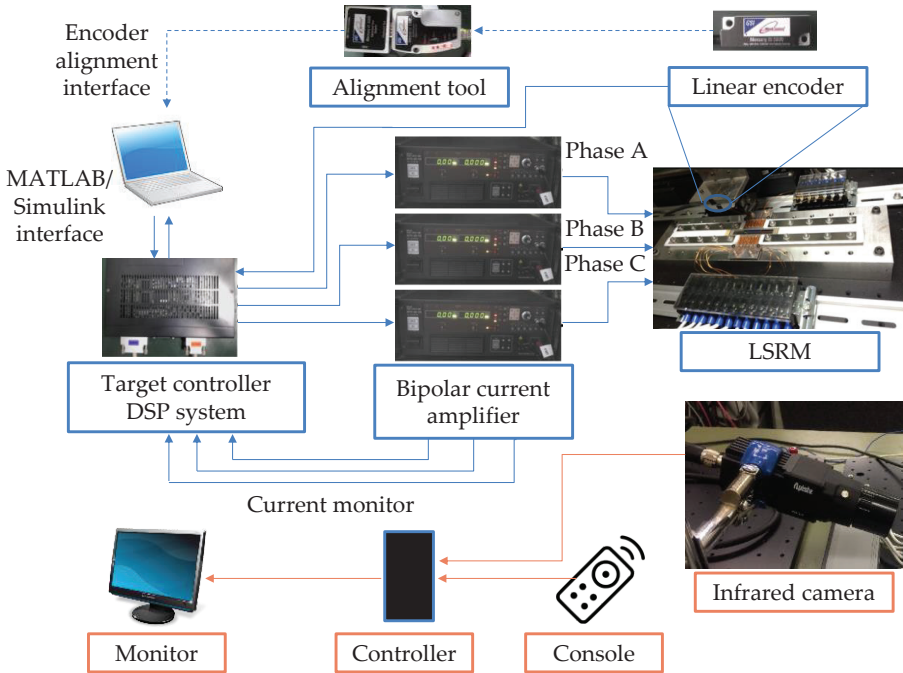
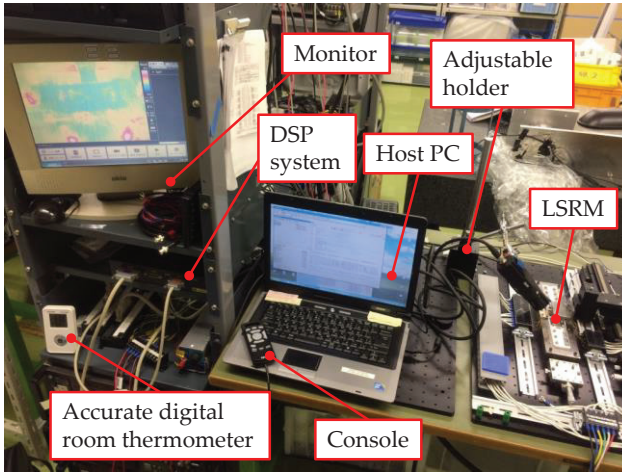
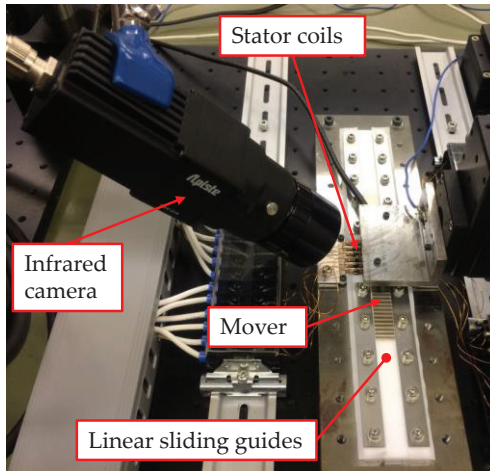


Figure 1: Schematic diagram of the experimental setup

Figure 2(a) shows the overall view of the experimental setup, while Figure 2(b) shows the zoomed view of the LSRM prototype and the thermography equipment. The mover used is the same as in previous study. It is placed on the sliding surface that is bonded with a low-friction polytetrafluoroethylene (PTFE) film between the stator coils. The displacement of the mover is obtained using a linear encoder (Mercury II 5800 by GSI Group Inc.) mounted above the motor. Meanwhile, the temperature information is obtained using an infrared camera (FSV-2000, Apiste Corporation) at a frame rate of 5 frames per second (fps). An accurate digital room thermometer is placed near the experimental setup to measure the room temperature.



(a)

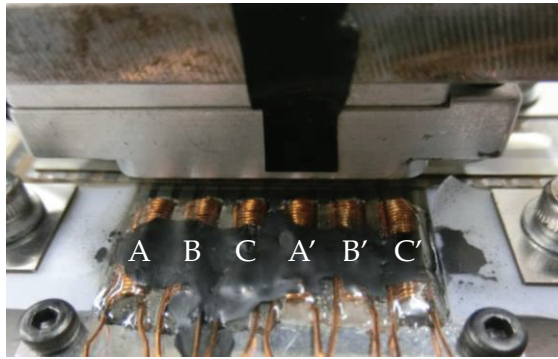


(b)

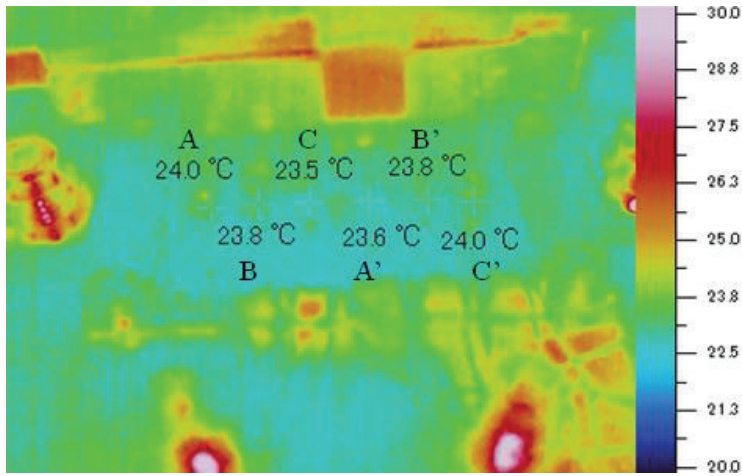
Figure 2: (a) Overall view of the experimental setup and (b) zoomed view of the LSRM prototype and the thermography equipment

## 2.2 Experimental Conditions

Figure 3(a) shows the field of view of the infrared camera. The field of view covers one side of stator coils where the three-phase coils (phases A, B and C) are located. A part of the coils is covered with high emissivity paint. The infrared camera is fixed at an angle to provide an accurate measurement of the temperature. As can be seen in Figure 3(b), the temperature distribution among the coils is similar when the motor is not in operation.



(a)



(b)

Figure 3: (a) Field of view of the infrared camera and (b) measured temperature distribution

### 3.0 RESULTS AND DISCUSSION

Three experimental cases were conducted depending on the input signal. The stator coils were cooled to near room temperature before beginning each experiment. The room temperature was 24.5 °C. For the first two cases, the response to a sinusoidal input of 3 mm amplitude at 0.25 Hz was measured. Figures 4(a) and 5(a) show the response of the motion control system running continuously for 6 and 30 s, respectively. As can be seen in Figures 4(b) and 5(b), the temperatures of the coils increased gradually to approximately 25 and 27 °C, respectively. They were increased gradually within the experimental period, or the period when the motion control system was running continuously. The temperature rise in the stator coils during motion is smaller than 3 °C.

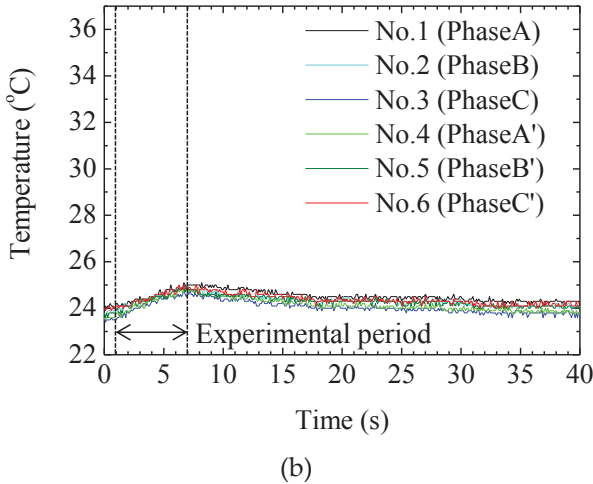
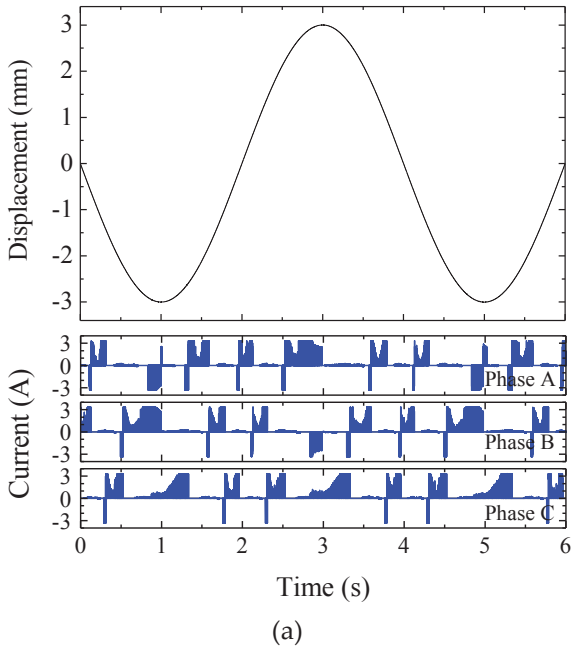
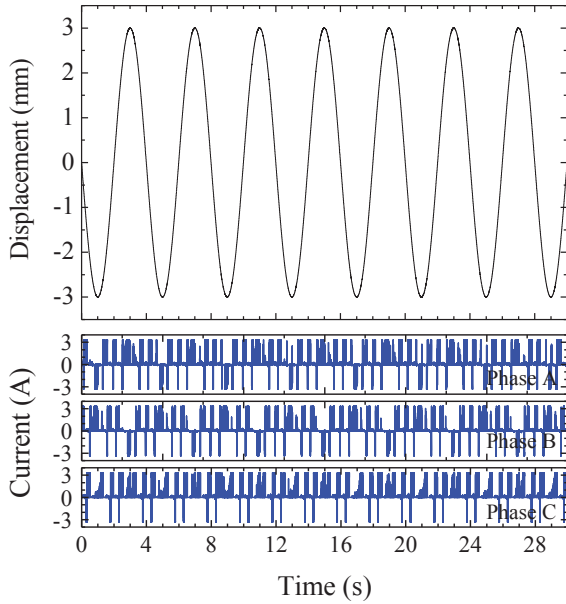
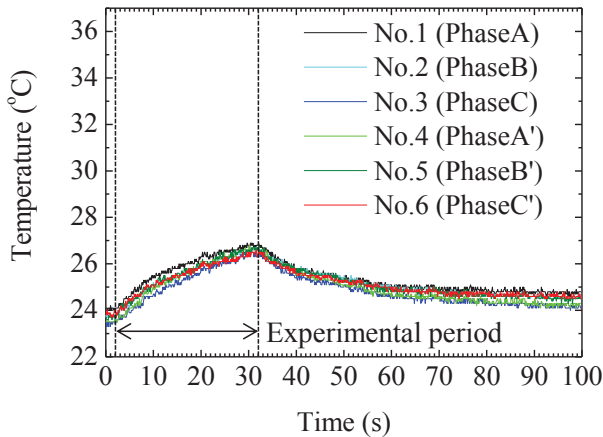


Figure 4: (a) Response of the motion control system for a sinusoidal input (3 mm, 0.25 Hz) running continuously for 6 s and (b) measured temperature by the thermography running continuously for 6 s



(a)



(b)

Figure 5: (a) Response of the motion control system for a sinusoidal input (3 mm, 0.25 Hz) running continuously for 30 s and (b) measured temperature by the thermography running continuously for 30 s

Meanwhile, for the last remaining case, Figure 6(a) shows the current responses of 3.33 A continuously applied to the coils. To simulate the worst case, the linear encoder to detect the displacement of the mover was turned off. Figure 6(b) shows the measured temperature of the LSRM using the above-mentioned input. In contrast with the first two cases, the temperature rises to its maximum of approximately 36 °C

within the experimental period resulting from such input signal for the worst case of operation. Overall, the temperature rise in the stator coils was about 12 °C and 4 times as large as that in coils during motion.

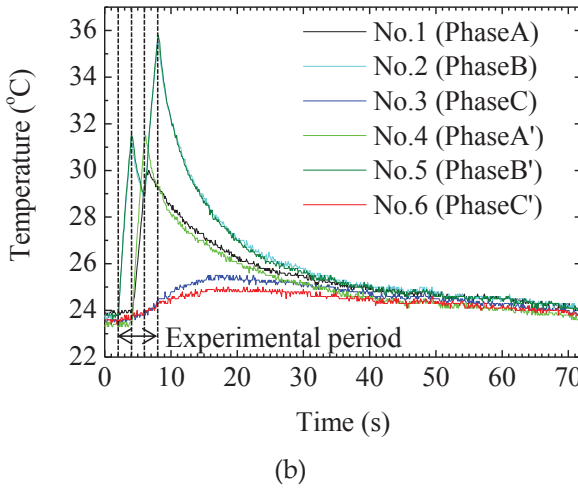
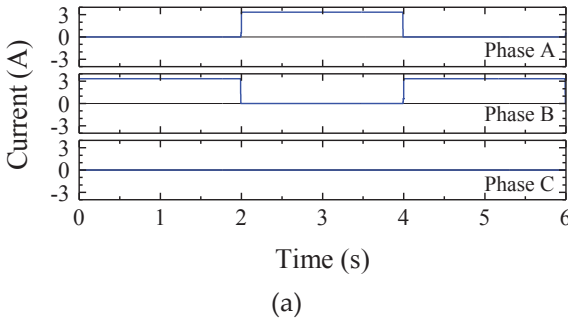


Figure 6: (a) Current responses of 3.33 A continuously applied to the coils and (b) measured temperature by the thermography when a current of 3.33 A was continuously applied to the coils

Overall, continuous motion longer than 30 s increases the temperature of the LSRM only by less than 3 °C. It was reported that similar motion experiments increase the temperature by up to 6 °C using the moving PM linear synchronous motor [1]. The experimental results indicate and highlight the key advantage of LSRMs that have less thermal problems compared with PM linear motors. This is a result of their simple and robust construction without PMs [10].



## 4.0 CONCLUSION

In this paper, the temperature characteristics of a thin and compact LSRM was presented. As the temperature change is undesirable for the motor, as its use for high-precision positioning and motion, the temperature rise in the stator coils during motion were examined experimentally. The temperature distribution among the coils are well expected, having similar temperatures when the motor is in operation or not. During typical operation of the motor by the motion control system running continuously for 30 s, the temperature of the stator coils is less than 27 °C. Hence, the temperature rise in the stator coils during motion is only smaller than 3 °C.

## ACKNOWLEDGMENTS

This work is supported by the fund for the Mikiya Science and Technology Foundation and has been done in the Kaiji Sato Laboratory, Tokyo Institute of Technology, Japan.

## REFERENCES

- [1] K. Sato, "High-precision and high-speed positioning of 100G linear synchronous motor", *Precision Engineering*, vol. 39, pp. 31–37, 2015.
- [2] W.C. Gan, N.C. Cheung and L. Qiu, "Position control of linear switched reluctance motors for high-precision applications", *IEEE Transactions on Industry Applications*, vol. 39, no. 5, pp. 1350–1362, 2003.
- [3] H.K. Bae, B.S. Lee, P. Vijayraghavan and R. Krishnan, "A linear switched reluctance motor: converter and control", *IEEE Transactions on Industry Applications*, vol. 36, no. 5, pp. 1351–1359, 2000.
- [4] G. Baoming, A.T. de Almeida and F.J. Ferreira, "Design of transverse flux linear switched reluctance motor", *IEEE Transactions on Magnetics*, vol. 45, no. 1, pp. 113–119, 2009.
- [5] B.S. Lee, H.K. Bae, R. Krishnan and P. Vijayraghavan, "Design of a linear switched reluctance machine", *IEEE Transactions on Industry Applications*, vol. 36, no. 6, pp. 1571–1580, 2000.
- [6] J.F. Pan, Y. Zou and G. Cao, "An asymmetric linear switched reluctance motor", *IEEE Transactions on Energy Conversion*, vol. 28, no. 2, pp. 444–451, 2013.

- [7] D. Wang, X. Du, D. Zhang and X. Wang, "Design, optimization, and prototyping of segmental-type linear switched-reluctance motor with a toroidally wound mover for vertical propulsion application", *IEEE Transactions on Industrial Electronics*, vol. 65, no. 2, pp. 1865–1874, 2017.
- [8] S. Masoudi, M.R. Feyzi and M.B.B. Sharifian, "Force ripple and jerk minimisation in double sided linear switched reluctance motor used in elevator application", *IET Electric Power Applications*, vol. 10, no. 6, pp. 508–516, 2016.
- [9] T. Hirayama, S. Yamashita and S. Kawabata, "Design and analysis of linear switched reluctance motor with coreless HTS excitation windings for ropeless elevator," in *IEEE 21st International Conference on Electrical Machines and Systems*, Jeju, South Korea, 2018, pp. 1879–1884.
- [10] H.S. Lim and R. Krishnan, "Ropeless elevator with linear switched reluctance motor drive actuation systems", *IEEE Transactions on Industrial Electronics*, vol. 54, no. 4, pp. 2209–2218, 2007.
- [11] F. Daldaban and N. Ustkoyuncu, "A novel linear switched reluctance motor for railway transportation systems", *Energy Conversion and Management*, vol. 51, no. 3, pp. 465–469, 2010.
- [12] L. Kolomeitsev, D. Kraynov, S. Pakhomin, F. Rednov, E. Kallenbach, V. Kireev, T. Schneider and J. Böcker, "Linear switched reluctance motor as a high efficiency propulsion system for railway vehicles," in *International Symposium on Power Electronics, Electrical Drives, Automation and Motion*, Ischia, Italy, 2008, pp. 155–160.
- [13] X. Huang, Z. Lin and X. Xiao, "Four-quadrant force control with minimal ripple for linear switched reluctance machines", *CES Transactions on Electrical Machines and Systems*, vol. 4, no. 1, pp. 27–34, 2020.
- [14] V.G. Sampath, K. Abhishek and N.C. Lenin, "Design, development and electromagnetic analysis of a linear switched reluctance motor for automatic door systems of railway carriages", *International Journal of Vehicle Structures & Systems*, vol. 8, no. 4, pp. 204–206, 2016.
- [15] A. Lachheb, J. Khediri and L. El Amraoui, "Modeling and performances analysis of switched reluctance linear motor for sliding door application," in *IEEE 15th International Multi-Conference on Systems, Signals & Devices*, Hammamet, Tunisia, 2018, pp. 1336–1341.
- [16] I. Mahmoud and H. Rehaouia, "Design and modeling of open-loop components for a biomedical application", *International Transactions on Electrical Energy Systems*, vol. 26, no. 10, pp. 2244–2258, 2016.

- [17] J. Lin, K.W.E. Cheng, Z. Zhang, N.C. Cheung, X. Xue and T.W. Ng, "Active suspension system based on linear switched reluctance actuator and control schemes", *IEEE Transactions on Vehicular Technology*, vol. 62, no. 2, pp. 562–572, 2013.
- [18] N.A. Anang, Z. Jamaludin, L. Abdullah, M. Maharof and M.H. Nordin, "Robust motion controller design for precise tracking of ball screw driven positioning system", *Journal of Advanced Manufacturing Technology*, vol. 12, no. 1(4), pp. 73–86, 2018.
- [19] L. Abdullah, S.C.K. Junoh, S.N.S. Salim, Z. Jamaludin, T.H. Chiew, N.A. Anang, Z. Retas and M.H. Nordin, "Evaluation on tracking performance of NPID triple hyperbolic and NPID double hyperbolic controller based on fast fourier transform (FFT) for machine tools", *Journal of Advanced Manufacturing Technology*, vol. 12, no. 1(4), pp. 25–38, 2018.
- [20] M.N. Maslan and K. Sato, "Motion system design of a thin and compact linear switched reluctance motor with disposable-film mover", *Journal of Advanced Mechanical Design, Systems, and Manufacturing*, vol. 12, no. 1, pp. 1–12, 2018.

